PROCEEDINGS, Seventeenth Workshop on Geothermal Reservoir Engineering
Stanford University, Stanford, California, January 29-31, 1992
SGP-TR-141

FRACTURE OPENING/ PROPAGATION BEHAVIOR AND THEIR SIGNIFICANCE ON PRESSURE-TIME RECORDS DURING HYDRAULIC FRACTURING

Takashi Kojima, Yasuhiko Nakagawa*
Koji Matsuki and Toshiyuki Hashida

Faculty of Eng., Tohoku Univ., Sendai 980
* Hitachi Tohoku Software,LTD.,Sendai 980

ABSTRACT

Hydraulic fracturing with constant fluid injection rate was numerically modelled for a pair of rectangular longitudinal fractures intersecting a wellbore in an impermeable rock mass, and numerical calculations have been performed to investigate the relations among the form of pressure-time curves, fracture opening/propagation behavior and permeability of the mechanically closed fractures. The results have shown that both permeability of the fractures and fluid injection rate significantly influence the form of the pressure-time relations on the early stage of fracture opening. Furthermore it has been shown that wellbore pressure during fracture propagation is affected by the pre-existing fracture length.

INTRODUCTION

Hydraulic fracturing is widely used for stimulating low permeability reservoirs in geothermal, oil and gas fields. In order to accomplish the fracturing job efficiently, it is desirable to know the fracture opening/propagation behavior and the permeability of the fracture during the job. In this study, in order to extract these information from pressure-time records during the hydraulic fracturing, the fracturing process was numerically simulated. Recent years, a number of mumerical studies for hydraulic fracturing were reported, for example, Lam et al.(1988), Vandamme et al.(1989) and Boone et al.(1990). However mostly the purposes were to design hydraulic fracturing and to estimate the fracture dimensions. Accordingly they assumed incompressible fluid flow, which is valid for the purposes, and didn't pay enough attention to pressure-time curves. For simulating a complete pressure-time curve, we must consider the compressibility of fluid. Numerical simulations, in which the compressibility of fluid was taken into account, were carried out by Hardy et al.(1989) and Ito et al.(1990), whose purpose was to investigate fracture reopening pressure for techtonic stress measurement with hydraulic fracturing. However these studies were restricted to the simulations of small scale fracturing.

In our numerical study, by taking the compressibility of fluid into account, the relations between fracture opening/propagation behavior and pressure-time curves were investigated. We numerically modelled the hydraulic fracturing conducted on a pair of pre-existing fractures intersecting a wellbore. This is the case often experienced in actual geothermal fields. In addition, permeability of the mechanically closed fractures were taken into account as one of parameters in the numerical calculations.

MATHEMATICAL FORMULATION OF THE PROBLEM

Consider a pair of pre-existing rectangular fractures intersecting a vertical wellbore in a rock mass which is assumed to be homogeneous, isotropic, linear elastic, infinite and impermeable. By injecting fluid with constant rate through the wellbore, the fractures open and propagate. The geometry of the hydraulic fracturing model is shown in Fig.1 with

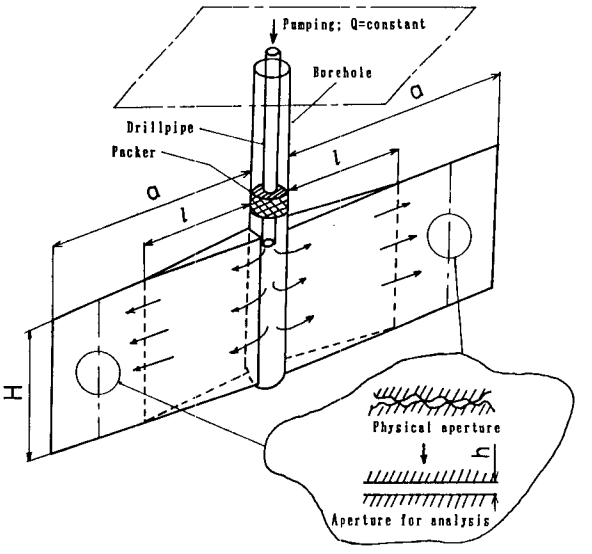

Fig.1. The model of hydraulic fracturing for numerical analysys.

symbols of dimensions we used. We made the following additional assumptions:

(1) The hight of the fractures is constant.

(2) Slippage at the top and the bottom of the fracture is allowed in the direction perpendicular to the fracture plane. Therefore the cross sectional area perpendicular to the direction of fracture propagation is rectangular in shape.

(3) There is no leak-off of the injection fluid. All the fluid is used for pressurization of the system (a drillpipe and a packed section of the wellbore) and the fractures.

(4) The fluid flow in the fractures are 1-D laminar flow parallel to the direction of fracture propagation.

(5) The flow rate at the tips of the fractures is zero.

(6) Although the fractures are mechanically closed, there are pore spaces available for fluid flow because of asperities at the surfaces. We substituted the physical aperture by the aperture h between smooth paralell walls (Fig.1). This aperture is equivalent to the physical aperture in permeability, and, here, is named hydromecanical aperture of a closed fracture.

From the above assumptions, the problem of fracture opening/propagation was reduced to a plane strain problem concerning with 2-D surface cracks emanating from a cylindrical cavity in an infinite elastic medium (Fig.2). Let (x,y) be the Cartesian

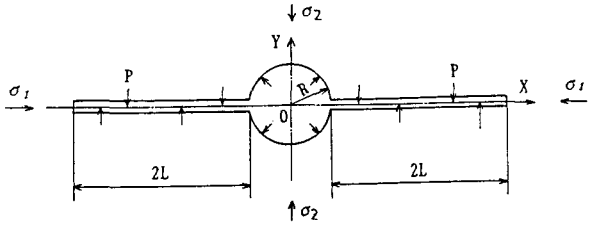

Fig.2. Two-dimensional modelling of fractures for stress / displacement analysis.

coordinate system with the origin at the center of the cavity, as shown in Fig.2. The cavity and the cracks are subjected to a fluid pressure $P(x)$ and the elastic medium is subjected to a biaxial compressive stress field (σ_1 and σ_2, $\sigma_1 > \sigma_2$) at infinity. R and $2L$ denote the radius of the cavity and the length of the cracks, respectively. In the analysis of fracture opening, $2L$ corresponds to fracture opening length l (Fig.1), and in the analysis of fracture propagation, it corresponds to fracture length a (Fig.1). Here, by using complex stress functions and the method of continuous distribution of edge dislocations, this problem comes to solving a singular integral equation of the Cauchy type (Hayashi et al., 1989), where the unknown function is the gradient of the crack opening displacement $b(x)$ along the crack line. The basic integral equation is:

$$\gamma \int_R^{R+2L} \{\frac{1}{x-\tau} + \frac{1}{R}K(x,\tau)\}b(\tau) = f(x), \qquad (R < x < R+2L), \tag{1}$$

where

$$K(x,\tau) = R\{-\frac{1}{x+\tau} + 2\frac{\tau^2-R^2}{\tau x^2} - \frac{\tau}{\tau x - R^2} + \frac{\tau}{\tau x + R^2} - \frac{\tau(\tau^2-R^2)}{(\tau x - R^2)^2} - \frac{\tau(\tau^2-R^2)}{(\tau x + R^2)^2} + \frac{R^2(\tau^2-R^2)^2}{\tau(\tau x - R^2)^3} - \frac{R^2(\tau^2-R^2)^2}{\tau(\tau x + R^2)^3}\}, \tag{2}$$

$$f(x) = \frac{1}{4}(\sigma_1+\sigma_2)(1+\frac{R^2}{x^2}) - \frac{1}{4}(\sigma_1-\sigma_2)(1+\frac{3R^4}{x^4}) - \frac{1}{2}(P(x)+\frac{R^2}{x^2}P(R)), \tag{3}$$

$$\gamma = \frac{G}{4\pi(1-\nu)}, \tag{4}$$

Here G and ν are shear modulus and Poisson's ratio, respectively. Crack opening displacement $w(x)$ and stress intensity factor K_I are given by:

$$w(x) = -\int_{R+2L}^{x} b(\tau)d\tau, \tag{5}$$

$$K_I = \lim_{x \to (R+2L)^+} \sqrt{2\pi(x-(R+2L))}\,\sigma_y = 4\sqrt{\pi L}\,\sigma_2 \phi(1), \tag{6}$$

where ϕ is a bounded function on the crack such that:

$$\frac{G}{4(1-\nu)\sigma_2} b(x) = \phi\left(\frac{x-L-R}{L}\right)\sqrt{\frac{x-R}{2L+R-x}}, \tag{7}$$

Let $W(x)$ denote the fracture width, which is given by adding the hydromechanical aperture h of the closed fractures to the crack opening displacement $w(x)$, as:

$$W(x) = h + w(x), \tag{8}$$

For the fluid flow in the fracture, the equation of continuity is:

$$\frac{\partial}{\partial t}(\rho W) + \frac{\partial}{\partial x}(\rho u W) = 0, \tag{9}$$

where ρ is the density of the fluid and u denotes the flow rate that is given by:

$$u = -\frac{W^2}{12\mu}\frac{\partial P}{\partial x}, \tag{10}$$

where μ is the fluid viscosity. For a fluid whose compressibility is β,

$$\frac{\partial \rho}{\partial t} = \rho\beta\frac{\partial P}{\partial t}, \qquad \frac{\partial \rho}{\partial x} = \rho\beta\frac{\partial P}{\partial x}, \tag{11}$$

Equations (9)-(11) lead to the following differential equation governing $W(x)$ and $P(x)$:

$$W\beta\frac{\partial P}{\partial t}+\frac{\partial W}{\partial t}=\frac{\partial}{\partial x}\left(\frac{W^3}{12\mu}\frac{\partial P}{\partial x}\right), \tag{12}$$

The initial and boundary conditions are:

$$P=P_0, \qquad W=h, \tag{13}$$

$$\left.\begin{aligned} &Q=Q_D+Q_C, && Q_D=\beta V_D\frac{\partial P}{\partial x}\Big|_{x=R}, \\ &Q_C=-\frac{HW^3}{6\mu}\frac{\partial P}{\partial x}\Big|_{x=R}, && \frac{\partial P}{\partial x}\Big|_{x=a}=0, \end{aligned}\right\} \tag{14}$$

where P_0 is the initial value of $P(x)$ and Q is the volumetric flow rate of the injected fluid, which is divided into Q_D used for pressurization of the system and Q_C for the fracture, and V denotes the volume of the system. From equations (12)-(14), the changes of the wellbore pressure $P(R)$ with time are obtained.

NUMERICAL PROCEDURE

The fracture opening/propagation and the fluid flow in the fractures were coupled numerically by an iteration loop for each fracture opening/propagation step t, as illustrated in Fig.3. First we estimate both the fracture width distribution W^t at the fracture opening(or propagation) length $2L^{t-1}+\Delta L$ and the time Δt required to an extention of opening(or propagation) length ΔL. Secondly using these estimated values and the implicit method, equation (12) is solved numerically to give the pressure distiribution P^t. Thirdly from P^t and equations (1)-(8), a stress intensity factor K_I and a temporary fracture width distribution W^* are obtained. Equation (1) was solved numerically using Causs-Jacobi integration formular (Erdogan, 1978). Finally comparing K_I with the fracture toughness of rock K_{IC}($K_{IC}=0$ for fracture opening) and comparing W^* with W^t, thier differences was checked. The maximum error allowed was 10^{-5} MPa m for $|K_{IC}-K_I|$and 0.01 for $|W^*-W^t|/W^t$. At the (j+1)th iteration the fracture width W_{j+1} is estimated by:

$$W_{j+1}=W_j+\lambda(W_j^*-W_j), \tag{15}$$

where λ is the relaxation parameter, which ranged from 0.5 to 0.7 in this study.

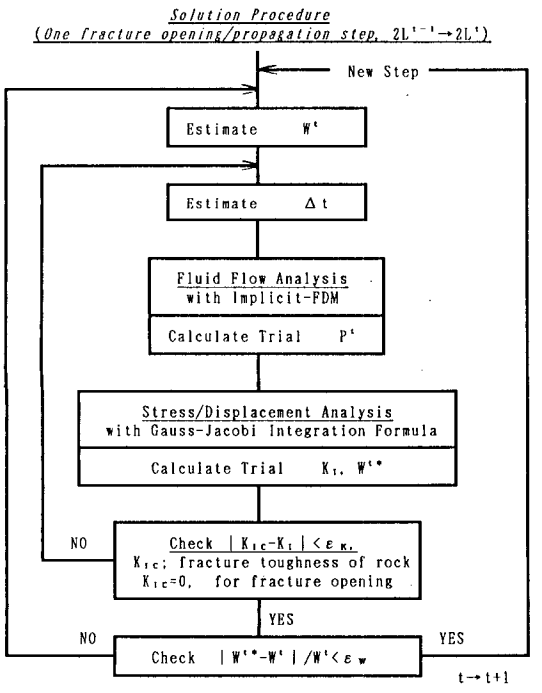

Fig.3. A flow chart of calculation procedure.

RESULTS AND DISCUSSION

Numerical calculations were performed to know the relations between fracture opening/propagation behavior and pressure changes with time by using the following values:
$\sigma_1=30$MPa, $\sigma_2=20$MPa, $P_0=10$MPa,
$G=3.5\text{X}10^4$MPa, $\beta=4.1\text{X}10^{-4}$MPa^{-1},
$\mu=5.5\text{X}10^{-10}$MPa·s
$R=0.682$m, $H=10$m, $V=3.0$m^3
The values associated with rocks were for hard rocks. In order to investigate the influences of both the fluid injection rate and the hydromechanical aperture of the closed fracture, Q and h were changed as $Q=10$, 100, 1000l/min and $h=10$, 500μm.

Opening Process of the Pre-exisiting Fractures

Fig.4 shows both the pressure-time curves and the change of fracture opening length with time for different hydromechanical aperture. In these calculations, the pre-existing fracture length a is long enough to be 1000m and Q is 100l/min. The pressure-time curves before the wellbore pressure reaches 17MPa aren't shown in the figures since the pressure-time curves are linear up to around 20MPa. The pressure at which the fractures begin to open is 15MPa in these cases. Therefore, it can be seen that the beginning of the fracture opening has no effect on the pressure-time curves, which is consistent with the result reported by Ito et al.(1990). When h is 10μm (Fig.4(a)), the wellbore pressure exhibits nonlinear increase with time from 20MPa to the maximum, 20.8MPa, and decreases gradually after the peak. On the other hand, when h is greater ($h=500\mu$m, Fig.4(b)), the wellbore pressure has no peak and becomes almost constant after it reaches about 20MPa which is equal to σ_2. Thus, the permeability of the closed fractures significantly affects the form of

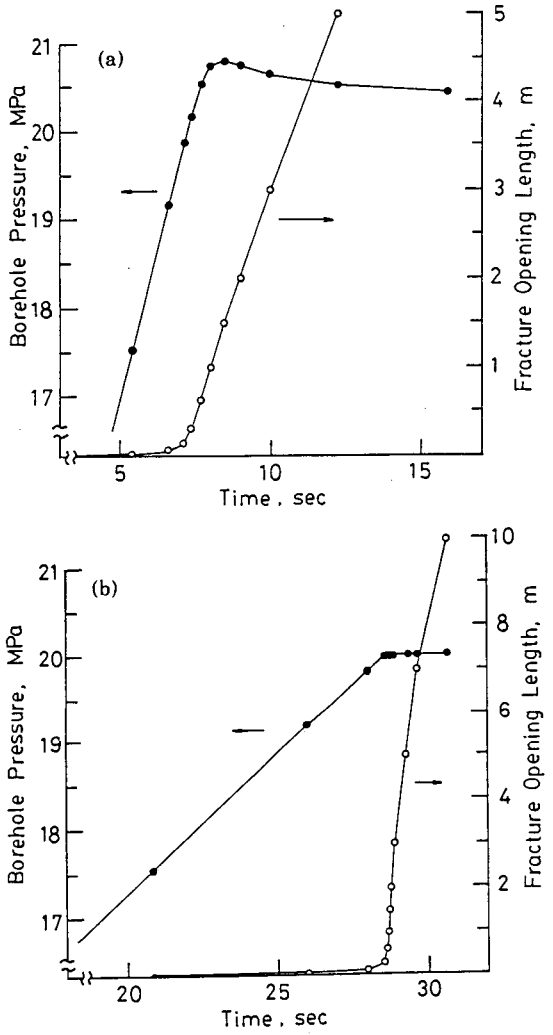

Fig.4. The change of borehole pressure and fracture opening length with time ((a) hydromechanical aperture $h=10\mu$m, (b) $h=500\mu$m).

pressure-time curves. Furthermore, from the change of fracture opening length with time, we can see that the fracture opening rate increases abruptly at the pressure, about 20MPa which is equal to σ_2.

As the peak in the pressure-time curves appear before the fracture opening length reaches 2m, let us look into the pressure distributions in the fracture within 2m from the wellbore surface (Fig.5). In the case of $h=10\mu$m, the pressure gradient in the opened portion is rather high owing to the low permeability of the closed portion, and the gradient begins to decrease from the wellbore side as the fractures open. In the case of $h=500\mu$m, on the other hand, the pressure gradient is fairly low due to the sufficiently high permeability. Figs.6(a) and 6(b) show the distributions of the fracture opening width, corresponding to Figs.5(a) and 5(b), respectively. The

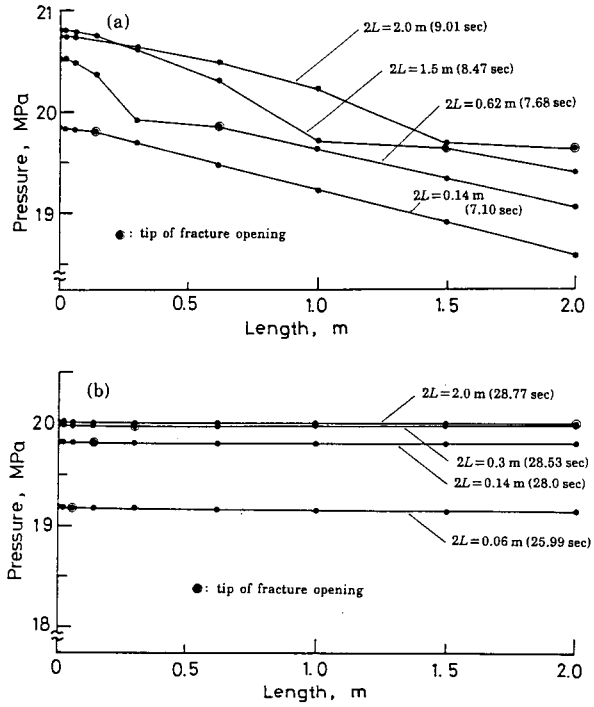

Fig.5. Pressure distribution in the pre-existing fracture during hydraulic fracturing ((a)hydromechanical aperture $h=10\mu$m, (b) $h=500\mu$m).

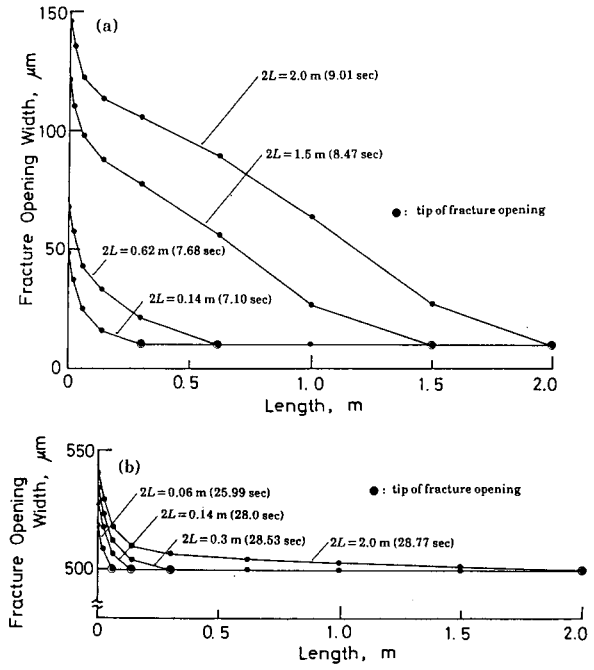

Fig.6. The distribution of fracture opening displacement during hudraulic fracturing ((a) hydromechanical aperture $h=10\mu$m, (b) $h=500\mu$m).

fracture opening displacements are greater in the case of $h=10\mu$m than those in the case of $h=500\mu$m because the pressure is much higher in the case of $h=10\mu$m. We can also see that in the case of $h=500\mu$m, the fracture opening displacement is considerably smaller than the hydromechanical aperture.

From Figs.5 and 6, we can now understand the reason for the differences in the form of the pressure-time curves shown Fig.4. When h is large, 500μm, because of the fairly low pressure gradient, the maximum pressure can not become significantly higher than 20MPa which is balanced with the normal stress acting across the fractures. On the other hand, when h is small, 10μm, the fluid pressure exceeds 20MPa at the wellbore in the early stage of fracture opening because of the higher pressure gradient. After that, by the further progression of fracture opening, the permeability and the volume of the aperture at the opened portion increase abruptly, and consequently the wellbore pressure begins to decrease. Thus, a clear peak appears in the pressure-time curves.

Fig.7 shows the influence of the hydromechanical aperture of the closed fractures on the pressure-time curves for various fluid injection rate, $Q=10$l/min, 100l/min and 1000l/min. In this figure, at the termination of each curves, the fracture opening length reaches 50m. As can be seen from the figure, both the permeability of the closed fractures and fluid injection rate have significant influence upon the form of pressure-time curves. The pressure-time curves have a peak only when the permeability is low enough, and the peak pressure becomes higher with the fluid injection rate. In adition, it is worthwhile to note here that in the case of $h=10\mu$m and $Q=1000$l/min, the pressure-time curve has a higher and sharper peak, whose form is similar to that of breakdown pressure which is observed at fracture initiation from a intact wellbore surface.

Fracture Propagation

Fracture propagations were simulated for the cases of pre-existing fracture length $a=1$m and $a=5$m, and the results are shown in Figs. 8(a) and 8(b), respectively. In these calculations, h, Q and K_{IC} were 10μm, 100l/min and 2.0MPa $\sqrt{\text{m}}$, respectively. In the case of $a=1$m, the pressure increases even after the fractures fully open and the pressure decreases soon after the fracture propagation. Accordingly the fracture propagation can be distinguished from the pressure-time curve. On the other hand, in the case of $a=5$m, the peak is induced only in the fracture opening process. As a consequence, it is difficult to distinguish the fracture propagation. By fracture mechanics consideration, it is obvious that the longer the pre-existing fracture length is, the lower the wellbore pressure which makes K_I of the fracture tip to be K_{IC}. Hence, it can be also concluded that for the pre-existing fracture whose length is greater than 5m, we can not know its propagation on the pressure-time cuve any longer.

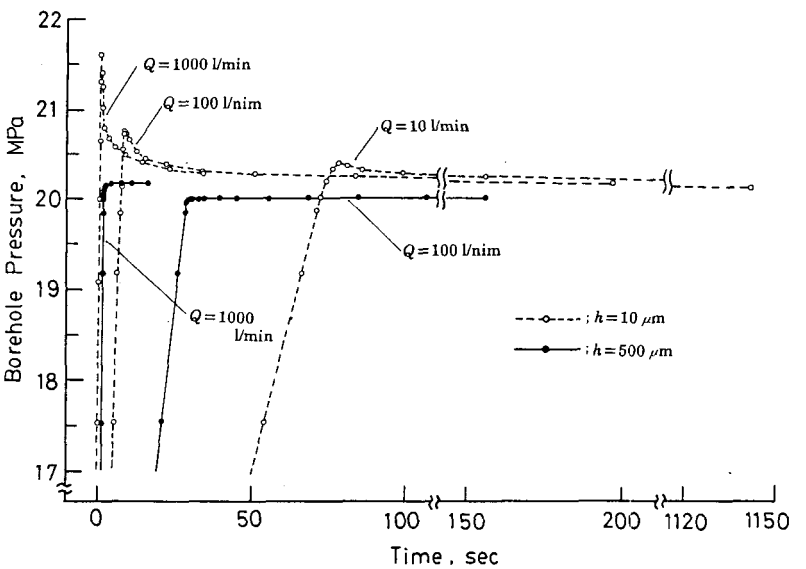

Fig.7. Influence of both permeability of fracture and fluid injection rate on pressure-time records during hydraulic fractureing.

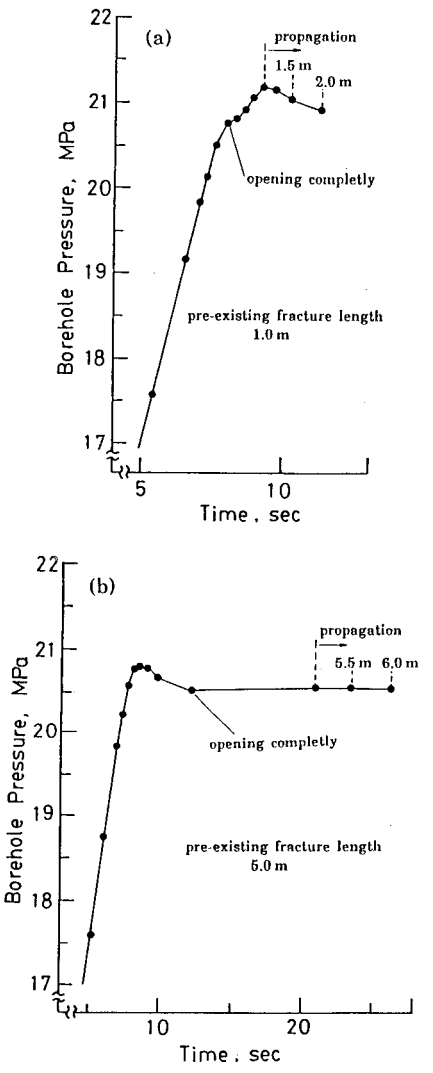

Fig.8. Influence of fracture propagation on pressure-time records during hydraulic fracturing ((a) pre-existing fracture length $a = 1$m, (b) $a = 5$m).

CONCLUDING REMARKS

In order to investigate the relations among fracture opening/propagation behavior, permeability of mechanically closed fracture and the form of pressure-time curves, hydraulic fracturing conducted on a pair of pre-existing fractures in a impermeable rock was numerically simulated and following results were obtained:

(1) Permeability of closed fracture affects significantly on the form of the pressure-time curves. When the permeability is sufficiently high, there is no peak in the pressure-time curves. On the other hand, when the permeability is low, the pressure-time curves have a peak, whose pressure becomes higher with the fluid injection rate.

(2) In the case of fracture propagation, wellbore pressure is influenced by the pre-existing fracture length. When the length is short enough, the pressure-time curves have the peak induced by the fracture propagation. On the other hand, when the length is long, the fracture propagation hardly influences the form of the pressure-time curves.

(3) In a series of hydraulic fracturing treatment, propping material injection for the sake of improving the fracture permeability is one of the important job. The dependence of the form of pressure-time curves on the permeability, which is shown in our results, shows that it is possible to judge the success of the job from the pressure-time records.

ACKOWLEDGMENT

The authors wish to thank Professors H.Abé, H.Takahashi and S.Suzuki, Faculty of Engineering, Tohoku University, for their encouragements throughout the course of the investigation. The authors also would like to acknowledge Pro. K.Hayashi, the Institute of Fluid Sience, Tohoku University, for his helpful advice.

REFERENCES

Boone,T.J. et al.(1990),"A Numerical Procedure for Simulation of Hydraulically-Driven Fracture Propagation in Porelastic Media," Int.J.Num.Anal.Methods Geomech., 14, 27-47

Erdogan,F.(1978),"Mixed Boundary-Value Problems in Mechanics," Mechnics Today, 4, 1-84

Hardy,M.P. et al.(1989),"Fracture Reopening during Hydrauric Fracuring Stress Determinations," Int.J.Rock Mech.Min.Sci.& Geomech.Abstr., 26, 489-497

Hayashi,K. et al.(1989),"Interpretation of Hydrauric Fracture Sut-in Curves for Tectonic Stress Measurement," Int.J.Rock Mech.Min.Sci.& Geomech.Abstr., 26, 477-482

Ito t. et al.(1991),"Theoretical Analysis of Crack Reopening Behavior in Hydraulic Fracturing Tectonic Stress Measurements," Transactions of the JSME, 57, 1715-1719

Lam,K.Y. et al.(1988),"Three-Dimensional Fracture Propagation under Specified Well-Bore Pressure," Int.J.Num.Anal.Methods Geomech., 12, 583-598

Vandamme,L. et al.(1989),"A Three-Dimentional Hydraulic Fracturing Simulator," Int.J.Num.Methods Eng., s28, 909-927